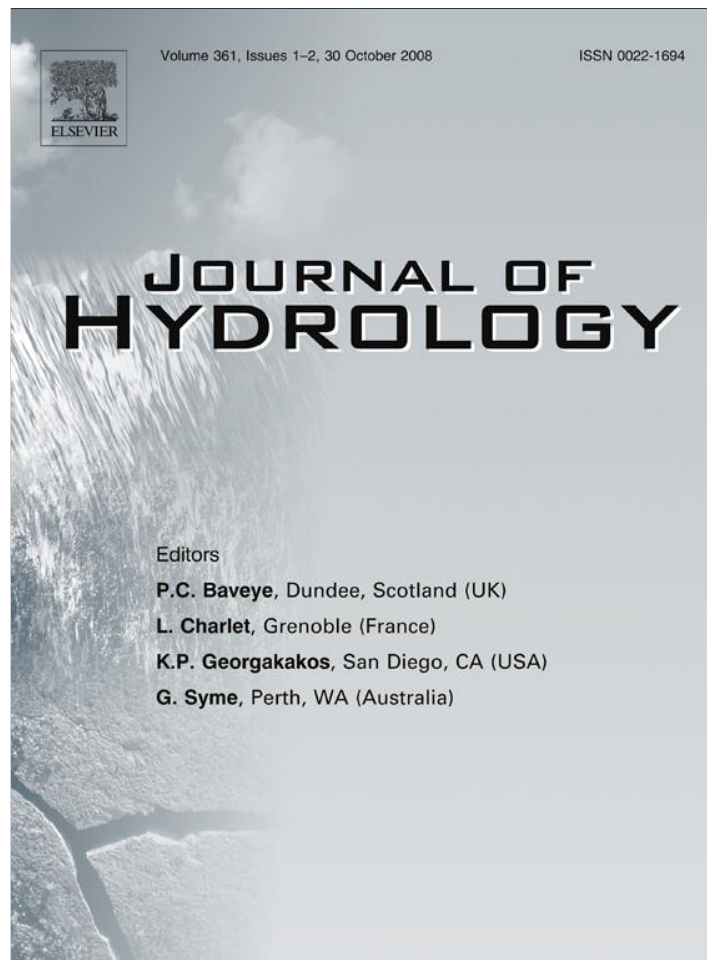


Provided for non-commercial research and education use.
Not for reproduction, distribution or commercial use.



This article appeared in a journal published by Elsevier. The attached copy is furnished to the author for internal non-commercial research and education use, including for instruction at the authors institution and sharing with colleagues.

Other uses, including reproduction and distribution, or selling or licensing copies, or posting to personal, institutional or third party websites are prohibited.

In most cases authors are permitted to post their version of the article (e.g. in Word or Tex form) to their personal website or institutional repository. Authors requiring further information regarding Elsevier's archiving and manuscript policies are encouraged to visit:

<http://www.elsevier.com/copyright>

available at www.sciencedirect.comjournal homepage: www.elsevier.com/locate/jhydrol

Evaluation of CO₂ fluxes from an agricultural field using a process-based numerical model

Jens S. Buchner ^{a,*}, Jiří Šimůnek ^a, Juhwan Lee ^b, Dennis E. Rolston ^c,
Jan W. Hopmans ^c, Amy P. King ^c, Johan Six ^b

^a Department of Environmental Sciences, University of California Riverside, Riverside, CA 92521, United States

^b Department of Plant Sciences, University of California, Davis, CA 95616, United States

^c Department of Land, Air and Water Resources, University of California, Davis, CA 95616, United States

Received 28 December 2007; received in revised form 18 July 2008; accepted 23 July 2008

KEYWORDS

Numerical model;
Carbon dioxide;
Uncertainty analysis;
Soil respiration;
SOILCO₂;
HYDRUS-1D

Summary During 2004, soil CO₂ fluxes, and meteorological and soil variables were measured at multiple locations in a 30-ha agricultural field in the Sacramento Valley, California, to evaluate the effects of different tillage practices on CO₂ emissions at the field scale. Field scale CO₂ fluxes were then evaluated using the one-dimensional process-based SOILCO₂ module of the HYDRUS-1D software package. This model simulates dynamic interactions between soil water contents, temperature, and soil respiration by numerically solving partial–differential water flow (Richards) and heat and CO₂ transport (convection–dispersion) equations using the finite element method. The model assumes that the overall CO₂ production in the soil profile is the sum of soil and plant respiration, whose optimal values are affected by time, depth, water content, temperature, and CO₂ concentration in the soil profile. The effect of each variable is introduced using various reduction functions that multiply the optimal soil CO₂ production. Our results show that the numerical model could predict CO₂ fluxes across the soil surface reasonably well using soil hydraulic parameters determined from textural characteristics and the HYDRUS-1D software default values for heat transport, CO₂ transport and production parameters without any additional calibration. An uncertainty analysis was performed to quantify the effects of input parameters and soil heterogeneity on predicted soil water contents and CO₂ fluxes. Both simulated volumetric water contents and surface CO₂ fluxes show a significant dependency on soil hydraulic properties.

© 2008 Elsevier B.V. All rights reserved.

* Corresponding author. Address: Institute of Environmental Physics, University of Heidelberg, Im Neuenheimer Feld 229, D-69120 Heidelberg, Germany. Tel.: +49 175 147 40 60; fax: +49 1212 5 13058642.

E-mail addresses: jens.buchner@iup.uni-heidelberg.de (J.S. Buchner), jiri.simunek@ucr.edu (J. Šimůnek).

Nomenclature

Numbers in parenthesis give the equation number when first used

α	empirical constants (reciprocal value of the air-entry value) (cm^{-1})
A_d	daily temperature amplitude ($^{\circ}\text{C}$) (3)
b_1, b_2, b_3	empirical constants (soil thermal conductivity) ($\text{J d}^{-1} \text{cm}^{-2} \text{K}^{-1}$) (2)
c_a, c_w	CO_2 concentration in the air and water phase ($\text{cm}^3 \text{cm}^{-3}$), respectively (4)
C_n, C_o, C_w, C_a	volumetric heat capacity of solid state, organic matter, water, and air phase, respectively ($\text{J cm}^{-3} \text{K}^{-1}$) (2)
D_{as}, D_{ws}	CO_2 diffusion coefficients of the air and water phase ($\text{cm}^2 \text{d}^{-1}$), respectively (4)
E	activation energy ($\text{kg cm}^2 \text{d}^{-2} \text{mol}^{-1}$) (7)
h	pressure head (cm) (1)
$h_1, h_2, h_3, h_4, h_2^*, h_3^*$	empirical constants (root water uptake) (cm)
k	number of executions of SOILCO2 (9)
K	hydraulic conductivity (cm d^{-1}) (1)
K_s	saturated hydraulic conductivity (cm d^{-1})
K_H	Henry's law constant ($\text{mol d}^{-2} \text{kg}^{-1} \text{cm}^{-1}$) (4)
K_m	Michaelis constant (–)
l	turtousity (–)
L_b	z-coordinate of the bottom of the soil profile (cm)
L_m, L_o	maximum and initial rooting depth (cm), respectively
L_r	rooting depth (cm)
L_u	z-coordinate of the soil surface (cm)
m	number of array entries (9)
n	empirical constant (shape parameter) (–)
N	degree days to maximum production ($^{\circ}\text{C}$)
p	porosity ($\text{cm}^3 \text{cm}^{-3}$) (4)
p_{ij}	random number weight factor (9)
Q, Q^*, S	source/sink terms (d^{-1}) (1) (4)
q_0	net surface flux (cm d^{-1})

q_c, \bar{q}_c	surface CO_2 flux and averaged surface CO_2 flux ($\text{cm}^3 \text{cm}^{-2} \text{d}^{-1}$), respectively (10)
q_w	water phase flux (cm d^{-1}) (2)
r	empirical constant (d^{-1})
R	universal gas constant ($\text{kg cm}^2 \text{d}^{-2} \text{K}^{-1} \text{mol}^{-1}$) (7)
RMSD	root mean square deviation
t	time (d) (1)
t_d	daily time (h) (3)
T	temperature (K) (2)
T_{20}	temperature that equals 20°C (k) (7)
T_d	daily average temperature ($^{\circ}\text{C}$) (3)
T_p	potential transpiration rate (cm d^{-1})
VWC	volumetric water content ($\text{cm}^3 \text{cm}^{-3}$)
$y, \Delta y, y'$	array of parameters, corresponding errors and varied parameters, respectively (9)
z	z-coordinate (cm) (1)
β_t	thermal dispersivity (cm) (2)
γ_{so}, γ_{po}	optimal CO_2 production by soil microorganism and plant roots (cm d^{-1}), respectively (5)
η	empirical constant (–) (8)
$\theta_n, \theta_o, \theta_a$	volumetric fraction of solid phase, organic matter and air phase ($\text{cm}^3 \text{cm}^{-3}$), respectively (2)
θ_w	volumetric water content ($\text{cm}^3 \text{cm}^{-3}$) (1)
θ_r, θ_s	residual and saturated water contents ($\text{cm}^3 \text{cm}^{-3}$), respectively
$\hat{\theta}_w, \tilde{\theta}_w$	averaged (spatially and for multiple runs) water contents ($\text{cm}^3 \text{cm}^{-3}$)
κ	empirical constant (d^{-1}) (8)
λ_w	dispersivity of the water phase (cm) (4)
$\sigma_{\theta_w}, \bar{\sigma}_{\theta_w}$	standard deviation and mean standard deviation of θ_w ($\text{cm}^3 \text{cm}^{-3}$) (11), (12)
$\sigma_{q_c}, \bar{\sigma}_{q_c}$	standard deviation and mean standard deviation of q_c (cm d^{-1})

Introduction

Concerns about rising atmospheric CO_2 levels and global climate change have motivated the investigation of strategies for promoting the sequestration of C in long-term storage pools. One of these potential pools, the soil organic carbon (SOC), is affected by a variety of agricultural management and land use strategies. Different cropping and tillage systems have been shown to have a significant impact on C dynamics (Paustian et al., 2000; Post and Kwon, 2000; McConkey et al., 2003; Osher et al., 2003).

Long-term land cultivation has contributed significantly to the observed global warming over the last 50 years at both the regional and global levels (IPCC, 2001, 2005). Since soil CO_2 accumulation and respiration play a major role in the global C cycle (Smith et al., 2003; Davidson and Janssens, 2006), the contribution of SOC to the entire climate system needs to be well understood. Different agricultural

management practices and land use have a significant impact on the behavior of the whole soil system and especially on soil C storage and greenhouse gas emissions (e.g., Paustian et al., 2000; Poch et al., 2005; Lee et al., 2006). Various environmental factors, such as soil temperature and water contents, simultaneously influence the microbial mediated release of CO_2 from soil C stocks (Fang and Moncrieff, 2001; Zak et al., 1999).

Using a holistic physical approach to better understand and describe the behavior of soil systems is of major interest in order to predict the contribution of soils to earth's water, CO_2 , chemical, and heat budgets. Of special interest for this purpose is the one-dimensional mathematical model SOILCO2 (Šimůnek and Suarez, 1993), which is built into the HYDRUS-1D software package (Šimůnek et al., 2005). HYDRUS-1D simulates spatial and temporal distributions of soil water, temperature, solutes, and CO_2 . Transport processes affecting these variables are described using nonlinear

partial-differential equations. The governing transport equations, such as the Richards equation for water flow and the convection-dispersion equations for heat, solute, and CO₂ transport are solved numerically using the finite element method. The contributions of various biological factors to CO₂ production (i.e., plant roots and microbiological organisms and respiration) are also considered in the model.

The SOILCO₂ model can be used for a wide range of temporal and spatial scales. The upper spatial limit is largely determined by uncertainty of input parameters due to their spatial heterogeneity, while the lower limit is given by the minimum scale at which the governing equations are valid. While SOILCO₂ can simulate short term (e.g., hourly or daily) CO₂ variations, the large majority of models simulating C and N turnover in soils, such as the DNDC (Li et al., 1992), CANDY (Franko et al., 1997), CENTURY (Parton et al., 1987, 1988, 1993), and RothC (Coleman and Jenkinson, 2005) are based on mass balance equations for finite soil layers and are designed for large spatial and long temporal scales. This enhances the applicability of these models in regional and global models but limits their use for studies of local processes. Recently, the SOILCO₂ model has received increased attention, and several of its applications have appeared in recent studies. For example, Herbst et al. (2008) coupled the SOILCO₂ model with a carbon turnover model and then successfully used the coupled model to simulate multiyear heterotrophic soil respiration from a bare soil experimental plot in Germany. Bauer et al. (2008) evaluated the sensitivity of simulated soil heterotrophic respiration to varying temperature and moisture reduction functions implemented in SOILCO₂.

In this paper, we evaluate soil CO₂ emissions from agricultural soils in the Sacramento Valley, California, using limited meteorological and soil information, and the one-dimensional process-based SOILCO₂ module of the HYDRUS-1D software package. The major objective of our investigations was to evaluate the performance of the SOILCO₂ model using typically collected information. Since measurements were not collected specifically for our model, both measured soil properties and literature values were used to parameterize the model. To quantitatively evaluate the impact of uncertainties of measured soil properties, a random value uncertainty analysis was carried out. Such analysis shows the capabilities and limits of the model, given its large demand on information and the one-dimensional representation of the soil domain.

Methods

Site description and data sampling

The experimental site is a 30-ha furrow irrigated agricultural field, located in the Sacramento Valley, near Winters, CA (38°36'N, 121°50' E). The slope of the field is less than 2%. The site was under observation using biweekly (growing season) and monthly (non-growing season) measurements of CO₂ emission, soil temperature, and volumetric water content during the period from 2003 until the middle of 2006 for predicting changes in landscape-scale soil organic C in a field recently converted from standard to minimum tillage

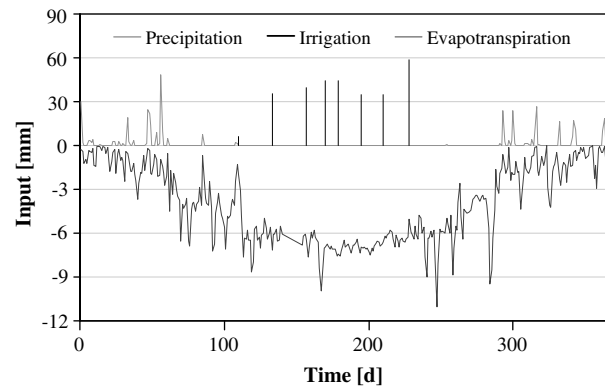


Figure 1 Mean daily values of precipitation, irrigation, and evapotranspiration. Please note the different scales for positive and negative values.

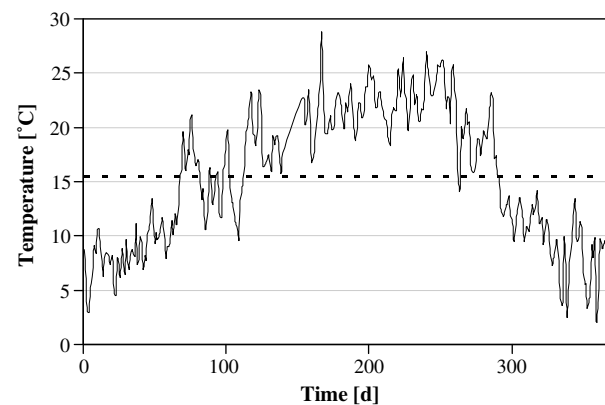


Figure 2 Mean daily (full line) and average annual (dotted line) air temperatures.

(Poch et al., 2005; Lee et al., 2006, 2007). The tillage and cropping history of the site was described in detail by Lee et al. (2007). In short, the field had been divided into two equal-sized areas in October 2003, and these were farmed using standard and minimum tillage. From April until September 2004, the field was cultivated with maize (*Zea mays* L.). For the modeling study presented in this paper, the time period from January 1 until December 31, 2004 was used.

Measurements of CO₂ emissions and relevant physical variables, such as precipitation, potential evaporation, air temperature, and volumetric water contents were carried out during this period. Figs. 1 and 2 present measured daily values of precipitation, irrigation, potential evapotranspiration, and air temperature. Meteorological data were obtained from the California Irrigation Management Information System CIMIS (<http://www.cimis.water.ca.gov/>).

In 2003, 30 plots for sampling of gases were established in the field. Two types of non-steady-state portable chambers that cover the soil surface only (no plants) were used. Insulated stainless steel chambers, which we moved from site to site and covered 0.012 m² of soil surface, were used from September 2003 through April 2004. In May 2004, 0.051 m² PVC rings were installed in the field. The rings

were pushed approximately 5 cm into the soil and placed at four different spots: the middle of the bed, the middle of the furrow, over the crop row but between plants (when applicable), and over the side dressed band (when applicable). Portable PVC end caps were converted into chamber lids, and placed on top of the rings for sampling. The CO₂ concentration inside the chambers was measured at 0, 30, 60, 120, 180, 240, and 300 s after placement of chambers over the soil surface with a Licor 6262 IRGA. The soil CO₂ flux was calculated using the measured CO₂ concentrations as input in the non-steady-state diffusive flux estimator model (Livingston et al., 2005, 2006). Measurements were taken at different times of the day at different locations. Since Lee et al. (2006) found little or no differences between CO₂ emissions from parts of the field with standard and minimum tillage, measurements from both sides of the field were combined in our analyses.

During each gas flux sampling, volumetric water content was measured using a portable time domain reflectometry probe (HydroSense, Decagon Devices Inc., Pullman, WA) over a depth interval from 0 to 12 cm. A field-specific calibration curve was generated using a polynomial regression of probe values to volumetric water contents (determined gravimetrically) for the top 0–12 cm.

Lee et al. (2007) also collected soil samples for measurements of soil texture in August 2003 (Table 1). The measurements were taken at 140 points in five depths (0–15, 15–30, 30–50, 50–75, and 75–100 cm). Bulk density, clay, silt, and loam percentages were averaged over all locations for a particular depth, as well as over the entire soil profile (Table 1). According to the USDA textural classification system, the soil can be categorized as being almost exactly on the boundary between loam and silt loam (Soil Conservation Service, 1972). The relatively large standard deviations reflect the high spatial variability of the measured soil physical properties across the field.

Numerical model

The SOILCO₂ model (Šimůnek and Suarez, 1993; Šimůnek et al., 2005) numerically simulates the movement of water, solutes, heat, and CO₂ in an arbitrary one-dimensional soil domain. The soil domain is represented by a spatial grid, in which every point can be assigned a certain soil type. Therefore, all functions representing physical variables can depend on both z and t , where z (cm) is the Euclidian coordinate orthogonal to the soil surface, and t (d) is time. The z -coordinate of the top and bottom of the soil column

are designated as L_u and L_b , respectively. The following description follows the work of Šimůnek and Suarez (1993). Note the notation section for definitions of various parameters.

Water movement

Water movement in a partially-saturated rigid porous medium, where the air phase is considered to be under constant atmospheric pressure, can be described using the following form of the Richards' equation:

$$\frac{\partial \theta_w}{\partial t} = \frac{\partial}{\partial z} \left[K \left(\frac{\partial h}{\partial z} - 1 \right) \right] - Q \quad (1)$$

where $\theta_w(h, z, t)$ is the volumetric water content ($\text{cm}^3 \text{cm}^{-3}$), $K(h, z, t)$ is the hydraulic conductivity (cm d^{-1}), $h(z, t)$ is the pressure head (cm), and $Q(h, z, t)$ is the root water uptake (d^{-1}). The two functions $\theta_w(h)$ and $K(h)$ can be described using the van Genuchten model (van Genuchten, 1980). These relations define soil hydraulic properties using six soil hydraulic parameters: residual water content θ_r , saturated water content θ_s , shape parameters α and n , saturated hydraulic conductivity K_s , and tortuosity and pore-connectivity parameter l .

The root water uptake function $Q(h, z, t)$ in Eq. (1) is a product of the potential transpiration rate $T_p(t)$ (cm d^{-1}), the function $\beta(z)$ (cm^{-1}) characterizing the spatial distribution of the root water uptake (Šimůnek et al., 2005), and the stress response function $\alpha(h)$. The time-dependent rooting depth, L_r , which affects the $\beta(z)$ function, is described using the Verhulst–Pearl growth function (Šimůnek and Suarez, 1993). The stress response function $\alpha(h)$ is defined following Feddes et al. (1978) using four empirical constants h_1 , h_2 , h_3 , and h_4 (cm) that characterize optimality of the root water uptake. The plant root water uptake model is therefore characterized by parameters T_p , L_m , L_0 , h_1 , h_2 , h_3 , and h_4 .

Atmospheric and free drainage boundary conditions are used at the upper and lower boundaries, respectively.

Heat transport

Heat transport can be described using the following convection–dispersion equation when the effects of the water vapor diffusion are neglected:

$$\begin{aligned} & (C_n \theta_n + C_o \theta_o + C_w \theta_w + C_a \theta_a) \frac{\partial T}{\partial t} \\ & = \frac{\partial}{\partial z} \left[(b_1 + b_2 \theta_w + b_3 \theta_w^{0.5} + \beta_t C_w |q_w|) \frac{\partial T}{\partial z} \right] - C_w q_w \frac{\partial T}{\partial z} \quad (2) \end{aligned}$$

Table 1 Percentages of clay, silt, and sand, bulk density (BD) and organic carbon content (C_{org}) for individual soil horizons averaged over all locations, as well as their average over the entire soil profile

Depth (cm)	Clay (%)	Silt (%)	Sand (%)	BD (g cm^{-3})	C_{org} (g m^{-3})
0–15	17.1 ± 3.1	51.5 ± 6.0	31.4 ± 8.7	1.04 ± 0.06	1220 ± 178
15–30	18.9 ± 3.4	53.5 ± 6.6	27.6 ± 9.6	1.37 ± 0.08	1215 ± 233
30–50	20.8 ± 3.7	52.8 ± 7.9	26.4 ± 10.1	1.51 ± 0.07	1025 ± 248
50–75	20.0 ± 4.1	51.7 ± 9.9	28.2 ± 13.4	1.58 ± 0.01	1092 ± 310
75–100	19.1 ± 4.4	48.3 ± 11.4	32.7 ± 15.16	1.58 ± 0.01	680 ± 357
0–100	19.3 ± 3.8	51.3 ± 8.8	29.4 ± 12.0	1.46 ± 0.04	1083 ± 311

Standard deviations of measured values are given after the '±' symbol. Measurements were taken in August 2003.

where C_i (J cm⁻³ K⁻¹) and $\theta_i(z, t)$ (cm³ cm⁻³) are volumetric heat capacities and volumetric fractions, respectively. The subscripts n, o, w, and a represent the mineral phase, organic matter, liquid phase, and air phase, respectively. In Eq. (2), $T(z, t)$ (K) and q_w (cm d⁻¹) represent temperature and water phase flux, respectively; b_1 , b_2 , and b_3 (J d⁻¹ cm⁻¹ K⁻¹) are empirical constants used in the function describing the dependency of the thermal conductivity on θ_w , and β_t (cm) is the thermal dispersivity. Hence, the soil thermal parameters C_n , C_o , C_w , C_a , θ_o , θ_n , b_1 , b_2 , b_3 , and β_t characterize the heat transport process.

Similarly as for water flow, the initial condition is given as the spatial temperature field $T(z)$ at $t = 0$ d. The upper boundary condition is specified as a Dirichlet boundary condition using the following sinusoidal function to represent daily variations of temperature at the soil surface:

$$T(t_d) = T_d(t) + A_d(t) \sin\left(\frac{2\pi t_d}{t_p} - \frac{7\pi}{12}\right), \quad z = L_u \quad (3)$$

Here, $T_d(t)$ (°C), $A_d(t)$ (°C), t_d (h), and t_p (=24 h) stand for the daily average temperature, daily temperature amplitude, day time, and day length, respectively. A Dirichlet boundary condition representing the annual average air temperature was used at the lower boundary.

Transport and production of carbon dioxide

In SOILCO₂, CO₂ transport is assumed to be caused by convection in the liquid phase, and diffusion in both the liquid and air phases. Furthermore, the gas phase is assumed to be stagnant, and the interaction of CO₂ with the soil matrix is neglected. The CO₂ concentrations in the water phase, c_w (cm³ cm⁻³), and in the air phase, c_a (cm³ cm⁻³), are linked using Henry's law (Šimůnek and Suarez, 1993).

The following convection–dispersion equation can then be used to describe the CO₂ transport:

$$\begin{aligned} & \frac{\partial(c_a\theta_a + c_w\theta_w)}{\partial t} \\ &= \frac{\partial}{\partial z} \left[\left(\theta_a D_{as} \frac{\theta_a^{7/3}}{p^2} \right) \frac{\partial c_a}{\partial z} + \theta_w \left(D_{ws} \frac{\theta_w^{7/3}}{p^2} + \lambda_w \left| \frac{q_w}{\theta_w} \right| \right) \frac{\partial c_w}{\partial z} \right] \\ & \quad - \frac{\partial}{\partial z} (q_w c_w) - Q^* + S \end{aligned} \quad (4)$$

where θ_a and θ_w (cm³ cm⁻³) are the volumetric contents of air and water phase, respectively, D_{as} and D_{ws} (cm² d⁻¹) are the diffusion coefficients of CO₂ in the gas and dissolved phases, respectively; p (cm³ cm⁻³) is the porosity and λ_w (cm) is the dispersivity in the water phase. The terms $Q^*(z, t)$ (cm³ cm⁻³ d⁻¹) and $S(z, t)$ (cm³ cm⁻³ d⁻¹) represent the sink/source terms for dissolved CO₂ in root water uptake and the CO₂ production by microorganisms and plant roots, respectively. The latter term is an important term of Eq. (4), as the CO₂ budget in the soil profile strongly depends on it. While volumetric water and air contents are expressed in units of volume of a particular phase divided by the volume of soil, CO₂ concentrations are defined in units of the CO₂ volume divided by the volume of the liquid or gas phase, respectively.

Initial conditions have to be provided for CO₂ concentrations, i.e., $c_a(z)$ at $t = 0$, similar to those for pressure heads and temperatures. The Dirichlet boundary condition with c_a equal to the atmospheric CO₂ concentration (=0.000379),

(IPCC, 2005) was used at the soil surface ($z = L_u$). At the lower boundary, a von Neumann boundary condition with zero concentration gradient was used since we expect a very low variability of the CO₂ concentration at the lower boundary.

The SOILCO₂ model assumes that CO₂ is produced by soil microorganism and plant roots, and that these two processes are additive (Šimůnek and Suarez, 1993). The model further assumes that the CO₂ production depends on several physical factors, and that the effect of these factors can be represented using the multiplication of appropriate functions. Hence,

$$S = \gamma_{s0} \prod_i f_{si} + \gamma_{p0} \prod_i f_{pi} \quad (5)$$

$$\prod_i f_i = f(z)f(h)f(T)f(c_a)f(t) \quad (6)$$

where subscripts s and p refer to soil microorganism and plant roots, respectively, γ_{s0} and γ_{p0} (cm³ cm⁻² d⁻¹, i.e., volume of CO₂ per unit area of the soil surface per unit time) are the optimal CO₂ production rates and f are individual reduction functions representing influence of various environmental factors.

Šimůnek and Suarez (1993) and Suarez and Šimůnek (1993) provided detailed description of all reduction functions used in Eqs. (5) and (6). But to further emphasize the importance of the temperature dependence of the CO₂ production, we give here only $f(t)$, which is assumed to be described by the Arrhenius equation as follows

$$f(T) = \exp\left[\frac{E(T - T_{20})}{RTT_{20}}\right] \quad (7)$$

where E (kg cm² d⁻² mol⁻¹) is the activation energy of the reaction, on which CO₂ production is based, R (kg cm² d⁻² K⁻¹ mol⁻¹) is the universal gas constant, and T_{20} (=293.15 K or 20 °C) is the reference temperature for the optimal production. It should be noted that from all reduction functions (6) only the function (7) can have values larger than one (for $T > T_{20}$) and thus an especially strong influence of the soil temperature on the CO₂ production is expected for these temperatures.

In summary, the transport of CO₂ is characterized fully by the set of transport parameters D_{as} , D_{ws} , and λ_w and the set of production parameters γ_{s0} , γ_{p0} , N , E , K_m , a^* , h_2^* , and h_3^* (see the Notation section for definitions). The default parameters discussed in Suarez and Šimůnek (1993) were used in the following simulations unless mentioned otherwise.

Selection of parameters, boundary and initial conditions

Proper selection of model parameters, characterizing different transport processes and factors, is of particular importance for the performance of the model and its simulation results. Whenever possible, the selection should be made based on measured data. However, when measured data have not been collected specifically for a particular model (the SOILCO₂ model in this case), external sources need to be used instead. The following section

Table 2 Soil hydraulic parameters determined using different methods: (A) neural network prediction using Rosetta (Schaap et al., 2001), (B) average parameters for the silt loam textural class (Cassel and Parrish, 1988), and (C) average parameters for the loam textural class (Cassel and Parrish, 1988)

Method	θ_r ($\text{cm}^3 \text{cm}^{-3}$)	θ_s ($\text{cm}^3 \text{cm}^{-3}$)	α (cm^{-1})	n	K_s (cm d^{-1})	l
A	0.062	0.386	0.007	1.59	11.28	-0.036
B	0.067	0.450	0.020	1.41	10.80	0.500
C	0.078	0.430	0.036	1.56	24.96	0.500

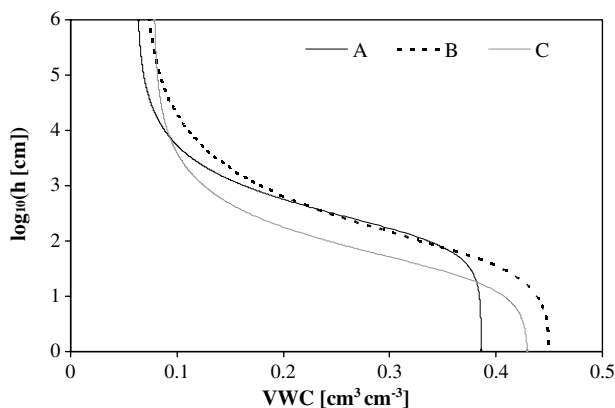


Figure 3 Retention curves corresponding to soil hydraulic parameters presented in Table 2. These parameters were obtained using (A) neural network predictions with Rosetta (Schaap et al., 2001), (B) average parameters for the silt loam textural class (Cassel and Parrish, 1988), and (C) average parameters for the loam textural class (Cassel and Parrish, 1988). VWC – volumetric water content.

discusses the set-up of the SOILCO2 model for this particular application and how required input parameters were obtained.

The 100-cm deep transport domain was described using a one-dimensional soil column with a spatial resolution of 1 cm. Two different ways were used to obtain the soil hydraulic parameters. First, the Rosetta module (Schaap et al., 2001) was applied using the data listed in Table 1 and assuming a vertically homogeneous soil profile. Second, average soil hydraulic parameters (Cassel and Parrish, 1988) were used for the soil textural classes classified according to the USDA system. Since the soil texture was categorized as almost exactly on the boundary between loam and silt loam, calculations were carried out using both textural classes. Three different sets of the soil hydraulic parameters and the corresponding retention curves are presented in Table 2 and Fig. 3, respectively.

The CIMIS data provides only potential evapotranspiration rates, ET_0 , which need to be divided into potential evaporation and potential transpiration rates for use in HYDRUS-1D. Therefore, the following logistic growth approach was used for this purpose:

$$T_p(t) = ET_0(t) \frac{\eta}{\eta + (1 - \eta) \exp(-\kappa t)} \quad (8)$$

where T_p is the potential transpiration (cm d^{-1}). The two empirical parameters ($\eta = 0.0001$ and $\kappa = 0.193 \text{ d}^{-1}$) were evaluated assuming that transpiration is, on average, 75%

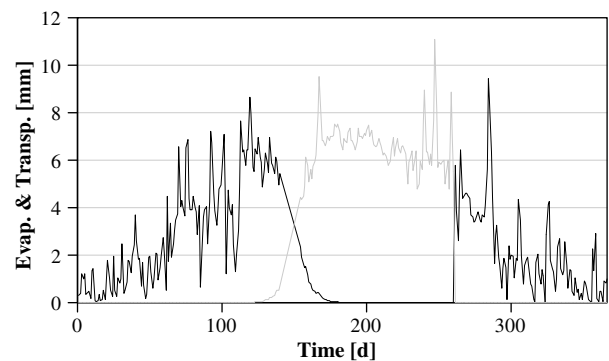


Figure 4 Mean daily values of potential evaporation (black line) and potential transpiration (grey line) during the simulation period.

of evapotranspiration during the entire growth period (Zhang et al., 2000). The evaporation rate is then given as a complementary value (Fig. 4). Since maize was planted in April, L_0 was set equal to zero. Dwyer et al. (1995) found maize's maximum rooting depth L_m to be 90 cm. The atmospheric boundary conditions are shown in Figs. 1 and 4.

Since no measurements of soil thermal parameters were carried out in the studied field, we used the default values of thermal capacities for individual soil phases, and the thermal conductivity function for silt, the dominant textural fraction (see Table 1). Soil thermal parameters used in HYDRUS-1D simulations are given in Table 3.

The upper boundary condition for heat transport calculations is defined for daily time t_d using average daily air temperatures, $T_d(t)$ (Fig. 2), and daily temperature amplitudes, $A_d(t)$ (Eq. (3)). Because of the lack of information about the bottom boundary, we used the mean air temperature, $T = 15.4 \text{ }^\circ\text{C}$, as the constant bottom boundary condition.

A comprehensive review of the selection of values for optimal CO_2 production, as well as coefficients for particular reduction functions, was provided by Suarez and Šimůnek (1993). The values for different reduction coefficients and optimal CO_2 production rates suggested in this review, which are implemented as default values in the HYDRUS-1D software package (Šimůnek et al., 2005), were used in the CO_2 transport and production model (Eqs. (5)–(7)). These coefficients, as well as coefficients describing root water uptake, are given in Table 3.

Since there were no specific measurements of initial conditions for $h(z)$, $T(z)$, and $c(z)$, we assumed a hydrostatic equilibrium for $h(z)$, and constant values for $T(z) = 15.4 \text{ }^\circ\text{C}$ and $c(z) = 0.000379 \text{ cm}^3 \text{ cm}^{-3}$.

Table 3 Parameters used in the model. Superscript numbers indicate literature source: (1) Taylor and Ashcroft (1972), (2) Chung and Horton (1987), (3) Patwardhan et al. (1988), (4) Suarez and Šimůnek (1993), (5) Holt et al. (1990), (6) www.wikipedia.org, (7) Šimůnek et al. (2005), (8) Maas (1990), (9) Buyanovski et al. (1986), and (10) Williams et al. (1972)

Root water uptake parameters				
h_1 (cm) ¹	h_2 (cm) ¹	h_{3u} (cm) ¹	h_{3l} (cm) ¹	h_4 (cm) ¹
-15	-30	-325	-600	-8000
Heat transport parameters				
C_n (J m ⁻³ K ⁻¹) ²	C_o (J m ⁻³ K ⁻¹) ²	C_w (J m ⁻³ K ⁻¹) ²	C_a (J m ⁻³ K ⁻¹) ²	
1.92×10^6	2.51×10^6	4.18×10^6	1.250×10^3	
b_1 (J s ⁻¹ m ⁻² K ⁻¹) ²	b_2 (J s ⁻¹ m ⁻² K ⁻¹) ²	b_3 (J s ⁻¹ m ⁻² K ⁻¹) ²	β_t (m) ²	
0.243	0.393	1.534	0.05	
CO ₂ production parameters				
D_{as} (cm ² d ⁻¹) ³	D_{ws} (cm ² d ⁻¹) ³	λ_w (m)	ρ (cm ³ cm ⁻³)	γ_{so} (cm ³ cm ⁻² d ⁻¹) ⁴
1.37376×10^4	1.529	Equal to β_t	Equal to θ_s	0.42
γ_{p0} (cm ³ cm ⁻² d ⁻¹) ⁵	N (°C) ⁶	E_p (kg cm ² d ⁻² mol ⁻¹) ⁷	E_s (kg cm ² d ⁻² mol ⁻¹) ⁸	
0.28	1360	6.48×10^{17}	7.19×10^{17}	
K_m^{*4}	a (cm ⁻¹) ⁹	h_2^* (cm) ¹⁰	h_3^* (cm) ¹⁰	
0.14	0.105	-100	-10 ⁶	

Table 4 Parameters and corresponding standard deviations used in the uncertainty analysis

θ_r (cm ³ cm ⁻³)	θ_s (cm ³ cm ⁻³)	α (cm ⁻¹)	n	K_s (cm d ⁻¹)	l
0.067	0.40	0.007	1.59	11.37	-0.044
$\Delta\theta_r$ (cm ³ cm ⁻³)	$\Delta\theta_s$ (cm ³ cm ⁻³)	$\Delta\alpha$ (cm ⁻¹)	Δn	ΔK_s (cm d ⁻¹)	Δl
0.008	0.02	0.001	0.04	3.87	0.128
b_1 (J s ⁻¹ m ⁻² K ⁻¹)	b_2 (J s ⁻¹ m ⁻² K ⁻¹)	b_3 (J s ⁻¹ m ⁻² K ⁻¹)			
0.154	-0.784	2714			
Δb_1 (J s ⁻¹ m ⁻² K ⁻¹)	Δb_2 (J s ⁻¹ m ⁻² K ⁻¹)	Δb_3 (J s ⁻¹ m ⁻² K ⁻¹)			
0.035	0.333	612			

Upper and lower four rows show hydraulic and selected thermal properties, respectively.

Parameter variation

As mentioned above, hydraulic properties and heat transport parameters were chosen or calculated based on the soil texture presented in Table 1. Large spatial variability of soil textural parameters produces uncertainty in predicted transport parameters, and consequently in model predictions. To evaluate the influence of this uncertainty on modeling results and study model sensitivity to these parameters, an uncertainty analysis was carried out.

For each parameter set, we defined an array y of selected input parameters and an associated array of errors Δy (Table 4), whereby each array consists of m entries. For each entry j , Δy_j is defined such that $2\Delta y_j$ matches the whole error range. While in section 'Model performance', the model is executed with only one array y , in the uncertainty analysis the model is executed a sufficient number of times (k) with the modified array y' to evaluate the model sensitivity to a particular parameter. The subscript i indicates each execution. The entries j of this array are given by

$$y'_{ij} = y_j + p_{ij}\Delta y_j \quad \forall j \in \{0, \dots, m\} \wedge i \in \{0, \dots, k\} \quad (9)$$

Weight factors p_{ij} ($-$) are normally distributed random numbers (Press et al., 1992) with a standard deviation that is equal to unity.

For the uncertainty analysis, the following quantities were defined. Averaging of simulated CO₂ fluxes, $q_{ci}(0, t)$ (cm³ cm⁻² d⁻¹), over all executions i gives mean CO₂ fluxes \tilde{q}_c (cm³ cm⁻² d⁻¹) and their corresponding standard deviations σ_{q_c} (cm³ cm⁻² d⁻¹):

$$\tilde{q}_c(0, t) = k^{-1} \sum_{i=0}^k q_{ci}(0, t) \quad (10)$$

$$\sigma_{q_c}(0, t) = \sqrt{(k-1)^{-1} \sum_{i=0}^k [q_{ci}(0, t) - \tilde{q}_c(0, t)]^2} \quad (11)$$

The mean standard deviation $\bar{\sigma}_{q_c}$ (cm³ cm⁻² d⁻¹) is obtained by averaging standard deviations σ_{q_c} over the simulation period as follows:

$$\bar{\sigma}_{q_c}(0) = (t_2 - t_1)^{-1} \int_{t_1}^{t_2} \sigma_{q_c}(0, t) dt \quad (12)$$

where t_1 and t_2 are the beginning time (=1 d) and the ending time (=366 d) of the simulation.

Similar definitions as those used for CO₂ fluxes in the three equations above, were also used for the volumetric water contents, $\theta_i(0, t)$.

Mean hydraulic parameters and their corresponding standard deviations used in the uncertainty analysis (Table 4) were obtained using the Rosetta model (Schaap et al., 2001) in combination with soil textural measurements (Table 1). Using mean values and standard deviations of the percentages of sand, silt, and clay, and bulk density (Table 1), new values of these variables were sampled 1000 times assuming that they are normally distributed. A new set of the soil hydraulic parameters was estimated using Rosetta for each new set of textural properties. These new sets were then evaluated to get their statistical parameters. This method, however, leads to a maximum coefficient of variations of 30% for K_s . This is small compared to the coefficient of variations of 120% reported by Nielsen et al. (1973). Hence, this latter value was used in the uncertainty analysis (Table 4) instead of the value provided by Rosetta. Mean values of the hydraulic parameters, and their corresponding standard deviations, presented in Table 4 are the result of these estimates.

A different method was used for soil thermal parameters. Chung and Horton (1987) provided thermal parameters only for clay, silt, and sand. While in direct calculations we used thermal parameters for silt, since silt is the main textural fraction, for the uncertainty analysis we calculated weighted averages and standard deviations of the three thermal parameters (Table 4) using the textural fractions (Table 1) as weighting.

3. Results and discussion

Model performance

Three simulation runs were performed with soil hydraulic properties obtained using the different methods (Table 2). Below, we present model results for the surface CO₂ flux, $q_c(0, t)$ (cm³ cm⁻² d⁻¹) and the volumetric water content averaged over the surface soil layer of 12 cm thickness:

$$\hat{\theta}_w(t) = \zeta^{-1} \int_0^\zeta \theta_w(z, t) dz \quad (13)$$

Here, $\theta_w(z, t)$ (–) is the volumetric water content as a function of depth and time, and $\zeta = 12$ cm.

Fig. 5 shows a comparison of spatially averaged measured and calculated volumetric water contents for the three different sets of soil hydraulic parameters, listed in Table 2. In general, higher water content values were measured after rainfall or irrigation events, while high potential evapotranspiration resulted in a decrease in water contents during time periods without precipitation or irrigation. As expected, simulated water contents depended mainly on climatic conditions for all three runs. Rainfall events (Fig. 1) and low potential evapotranspiration rates (Fig. 4) led to high soil water contents in the range of 0.18–0.38 cm³ cm⁻³ from day 0 to day 70. Light precipitation and increasing potential evapotranspiration rates led to values in the range of 0.10–0.25 cm³ cm⁻³ between days 70 and 250. Only irrigation events during the same time period led to higher water contents for short times. In the last time

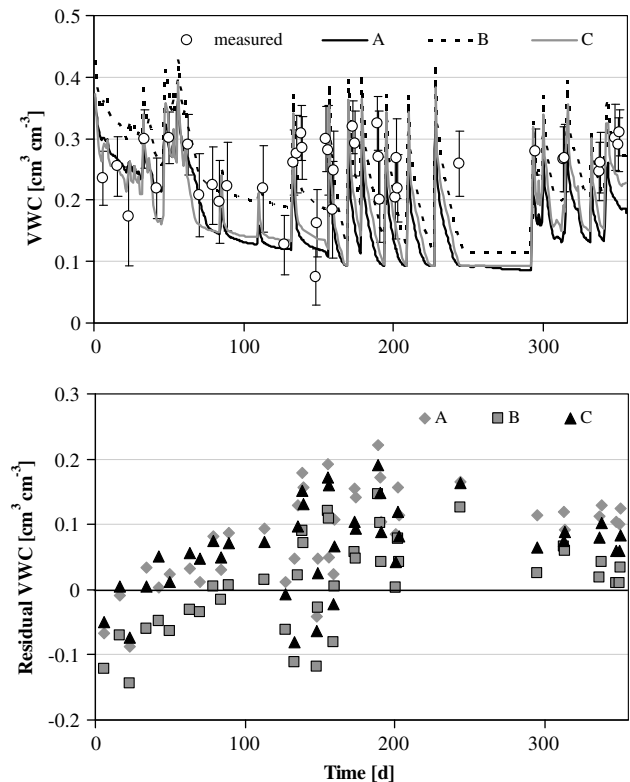


Figure 5 Measured and simulated volumetric water contents (VWC) (cm³ cm⁻³) averaged over the top soil layer at mean daily measurement times (top). Error bars represent one standard deviation resulting from spatial averaging. Residual (measured minus modeled) volumetric water contents (bottom). Cases A, B, and C are the same as in Fig. 3.

period (after day 250), moderate precipitation and decreasing evapotranspiration rates resulted in water contents in the range of 0.27–0.30 cm³ cm⁻³. Measured values are displayed with fairly large errors, indicating a high spatial variability across the field.

In all three runs, simulated values were in the same range as measured values. In run A, 32.5% of simulated values were in the error range of measured ones, while in runs B and C, 50.0% and 27.5% were in this range, respectively. Root mean square deviations (RMSD) were found to be 0.11, 0.07, and 0.09 cm³ cm⁻³, for A, B, and C, respectively. In addition, we observed coefficients of correlation of 0.19, 0.23, and 0.26. The best model performance was found for scenario B. The coefficients of correlation indicate a significant discrepancy between the modeled and measured values. The relative error of the water mass balance for model calculations was 0.076%, 0.102%, and 0.106% for case A, B, and C, respectively.

Fig. 6 presents measured and simulated soil temperatures at a depth of 5 cm. Simulation results for run A, B, and C were almost identical and thus are represented in the figure by a single line. Simulated values (31.6%) were in the error range of measured ones. The root mean square deviation (RMSD) and the coefficient of correlation were found to be 3.27°K and 0.90, respectively. Although these results and Fig. 6 show that the model can very well de-

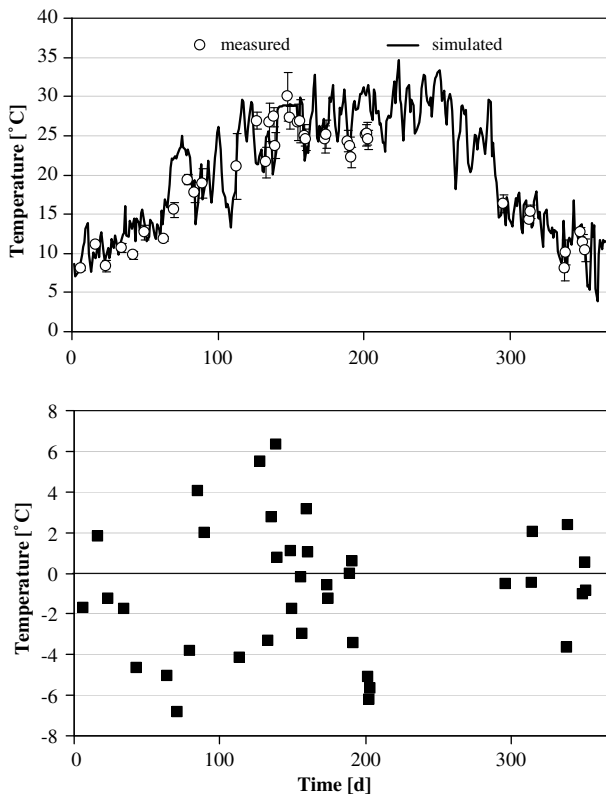


Figure 6 Measured and simulated soil temperatures at mean daily measurement times (top). Error bars represent one standard deviation resulting from spatial averaging. Residual (measured minus modeled) soil temperatures (bottom). Since results for runs A, B, and C were almost identical, they are represented by a single line. Both measured and simulated temperatures are given for a depth of 5 cm.

scribe the overall annual trend of soil temperatures, there are some differences for particular measurement times. There can be several reasons for this. Measurements across the entire field were taken over several hours (similarly as water contents) and then averaged. Measurements were taken with a digital thermistor at a 5-cm depth every time CO₂ flux measurements were taken and thus measurement depths and locations may have varied. Both these factors can lead to relatively unreliable values of measured temperatures.

Measured and simulated CO₂ fluxes as a function of time are presented in Fig. 7. There is one significant outlier measured at day 79, likely caused by a measurement error. The CO₂ efflux appears to display the same annual trend as air temperatures (Fig. 2), with the exception of the time period from day 100 to 150. This is likely due to low water contents during this time period, which led to reduction of soil CO₂ fluxes. High error ranges of CO₂ fluxes are partly due to a high spatial variability of water content values and partly due to different measurement times. Since measurements at different spots were typically taken during a time interval of 3 h, significant temperature differences could be observed between measurements at different locations. We also expect that there is a small contribution by the two

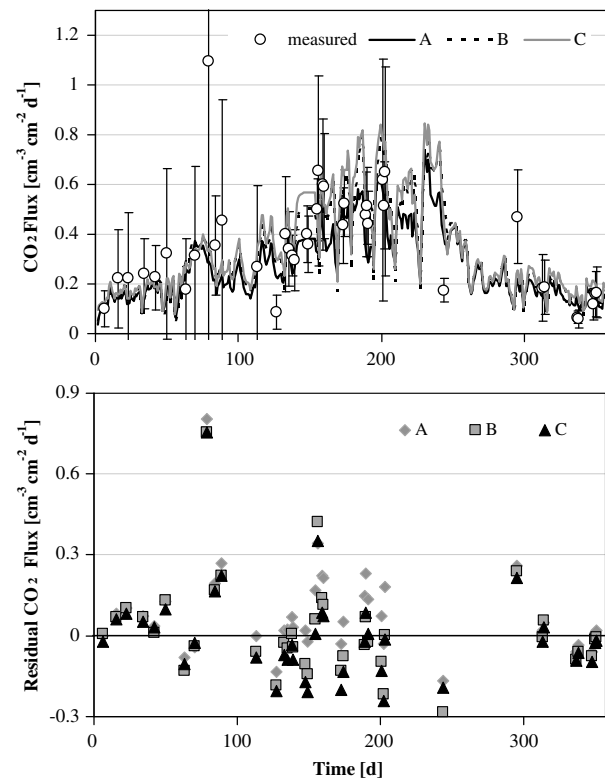


Figure 7 Measured and simulated CO₂ fluxes (cm³ cm⁻² d⁻¹) at mean daily measurement times (top). Error bars represent one standard deviation resulting from spatial averaging. Residual (measured minus modeled) CO₂ fluxes (bottom). Cases A, B, and C are the same as in Fig. 3.

different tillage practices to the high variability of observed CO₂ fluxes (Lee et al., 2006).

The correspondence between measured and simulated CO₂ fluxes was relatively good for all three simulation runs. Simulated values are within the error range of measured values in 80.0%, 77.5%, and 75% of cases for scenario A, B, and C, respectively. The large difference between measured and simulated CO₂ fluxes at day 295 is likely caused by the underestimation of the water content at the same time (Fig. 5).

A comparison of measured and simulated CO₂ fluxes (Fig. 7) with air temperatures (Fig. 2) shows the trend in the CO₂ efflux (using Eq. (7)) follows the annual temperature trend. Furthermore, irrigation events on days 133, 157, 170, 179, 196, 210, and 228 led to higher water contents, which should not limit CO₂ production by soil microorganisms. However, the CO₂ production by plant roots has been parameterized by the Feddes et al. (1978) function. Since irrigation events increase pressure heads (water contents) beyond their optimal range, the CO₂ production by plant roots decreases and so does the overall CO₂ production, because of the additive approach given by Eq. (5).

Fig. 8 presents a comparison of measured CO₂ fluxes and those calculated in the three runs. Coefficients of correlation were equal to 0.63, 0.59, and 0.60 in runs A, B, and C, respectively. The RMSD was found to be 0.18, 0.18, and 0.17 cm³ cm⁻² d⁻¹ for run A, B, and C, respectively.

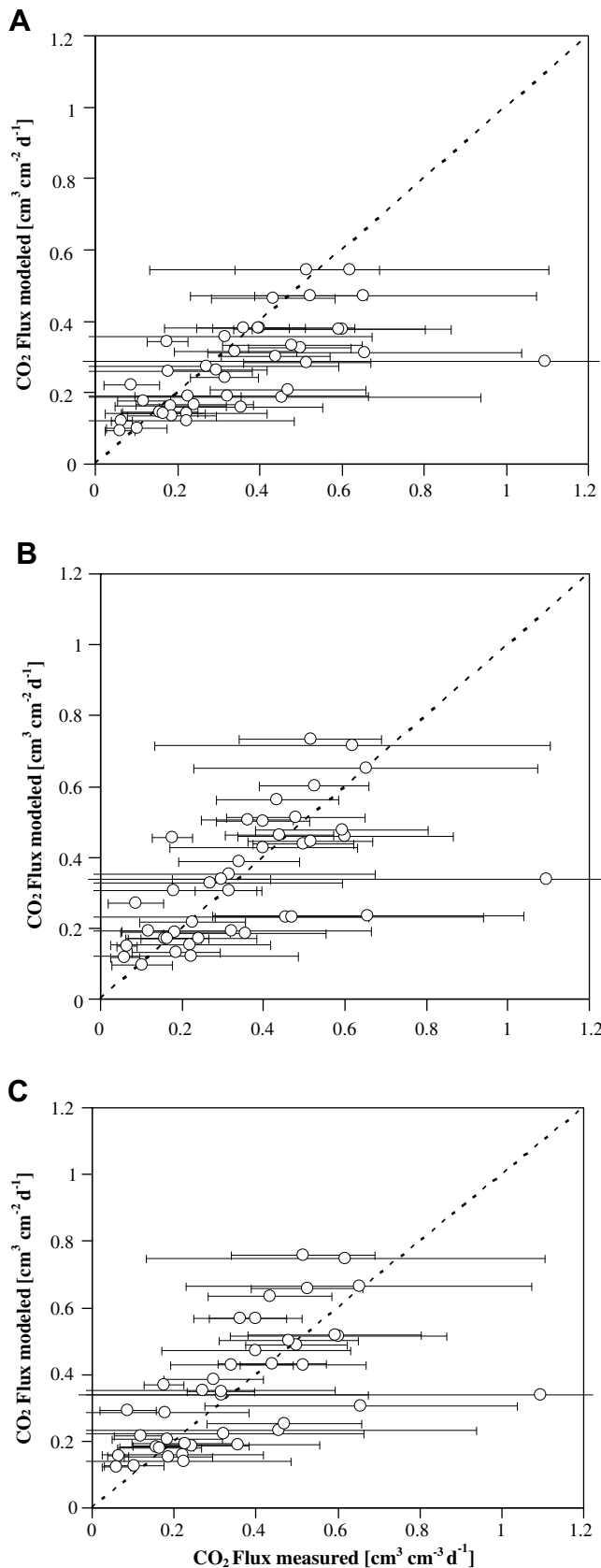


Figure 8 A comparison of measured and simulated CO₂ fluxes (cm³ cm⁻² d⁻¹). The dotted line represents 1:1 line. Error bars at measured values represent one standard deviation resulting from spatial averaging. Cases A, B, and C are the same as in Fig. 3.

However, 72.5%, 45%, and 40% of the data points can be found to the right of the 1:1 line for runs A, B, and C, respectively. This likely represents a certain structural underestimation of CO₂ fluxes by numerical simulations for case A, i.e., for the case when soil hydraulic parameters were estimated using Rosetta.

The modeled annual cumulative CO₂ fluxes were found to be 80.4, 93.8, and 99.2 cm³ cm⁻² for runs A, B, and C, respectively. These values correspond to 7.36×10^3 , 8.58×10^3 , and 9.08×10^3 kg ha⁻¹, respectively. The measured cumulative CO₂ efflux was found to be 118.2 ± 82.4 cm³ cm⁻² when using linear interpolation between measured values; this corresponds to $(10.81 \pm 7.5) \times 10^3$ kg ha⁻¹. The model thus underestimates the measured CO₂ flux by between 16% and 32%, while differences between particular model runs (A–C) are at most 20%. The maximum underestimation of the CO₂ efflux (37.8 cm³ cm⁻² in run A) is less than half the uncertainty of the measured value (82.4 cm³ cm⁻²).

It needs to be stressed here that this was achieved with an uncalibrated model, using mostly literature values. If we would have optimized selected parameters, such as γ_0 , the correspondence between measured and calculated values would have undoubtedly been much higher. However, it should also be stressed that 40 measurements during the entire season are likely not sufficient to provide a good estimate of the cumulative CO₂ flux. For example, [Parkin and Kaspar \(2004\)](#) stated that a sampling interval of 3 days is already linked with estimates of cumulative C loss within $\pm 20\%$ of the expected value. Sampling once every 20 d yielded potential estimates with +60% and -40% of the actual cumulative CO₂ flux.

Simulated volumetric water contents ([Fig. 5](#)), as well as CO₂ fluxes ([Fig. 7](#)), show a certain, although not particularly large, dependency on how the soil hydraulic parameters were selected. Even smaller is the effect of soil hydraulic parameters on simulated soil temperatures at a 5-cm depth ([Fig. 6](#)). The best predictions of volumetric water contents and CO₂ fluxes were obtained for runs A and B, respectively. However, the representation of a three-dimensional field scale soil domain using a one-dimensional model, and the characterization of the soil using an indirect estimate of the soil hydraulic properties, represent a considerable simplification of the problem that results in a loss of information. Furthermore, information about the lower boundary conditions for water flow, heat and carbon dioxide transport was not readily available, and hence simplified assumptions had to be made. As expected, certain discrepancies between measured and simulated volumetric water contents ([Fig. 5](#)) and CO₂ fluxes ([Figs. 7 and 8](#)) were found. For example, the model underestimated the total CO₂ fluxes by about 20%, which may thus hamper the applicability of the uncalibrated model. However, considering that all heat transport and CO₂ production and transport parameters used in the simulations were the default model parameters without any additional adjustments or fitting, acceptable correspondence between measured and simulated CO₂ fluxes ([Figs. 7 and 8](#)) documents the applicability of the SOILCO2 model (or HYDRUS-1D) for predicting CO₂ fluxes from agricultural soils under different climatic conditions at the field scale.

Uncertainty analysis

In the previous section, we found that there was a dependence of simulated results on soil hydraulic properties. In section 'Parameter variation' we derived average hydraulic and soil thermal parameters (Table 4) from measured soil textural components that have their corresponding uncertainties. To quantify the effects of these uncertainties, the following uncertainty analysis was performed.

Hydraulic and soil thermal parameters (Table 4) were modified separately using selected uncertainties, which were weighted with normally distributed random numbers (Eq. (9)). The SOILCO₂ model was executed 3000 times with a particular group of modified parameters.

Volumetric water contents simulated with modified hydraulic properties are shown in Fig. 9. Variations of soil hydraulic parameters, thermal transport parameters, and measurements resulted in the following mean standard deviations for the volumetric water content: $\bar{\sigma}_{\theta_w} = 4.28 \times 10^{-2}$, $\bar{\sigma}_{\theta_w} = 4.93 \times 10^{-5}$, and $\bar{\sigma}_{\theta_w} = 5.57 \times 10^{-2} \text{ cm}^3 \text{ cm}^{-3}$, respectively. Simulated CO₂ fluxes are presented in Fig. 10. Variations of soil hydraulic parameters, thermal transport parameters, and measurements produced the following mean standard deviations for CO₂ fluxes: $\bar{\sigma}_{q_c} = 4.90 \times 10^{-2}$, $\bar{\sigma}_{q_c} = 4.39 \times 10^{-3}$, and $\bar{\sigma}_{q_c} = 2.42 \times 10^{-1} \text{ cm}^3 \text{ cm}^{-2} \text{ d}^{-1}$, respectively.

Similar analysis was also carried out for other parameters, such as those affecting plant root water uptake and CO₂ production, using rather arbitrary estimates for their uncertainty ranges (since such information is not available). The impact of these uncertainties was of the same order or smaller than the impact of the uncertainty in the soil hydraulic parameters.

These results show that uncertainty in soil hydraulic properties has a much stronger impact on simulated volumetric water contents and CO₂ fluxes than uncertainty in soil thermal parameters. This is consistent with the model, since the volumetric water content directly influences CO₂ fluxes in several ways (Šimůnek and Suarez, 1993). Volumetric water contents affect directly the soil CO₂ respiration and indirectly the resistance to CO₂ flow by dramatically

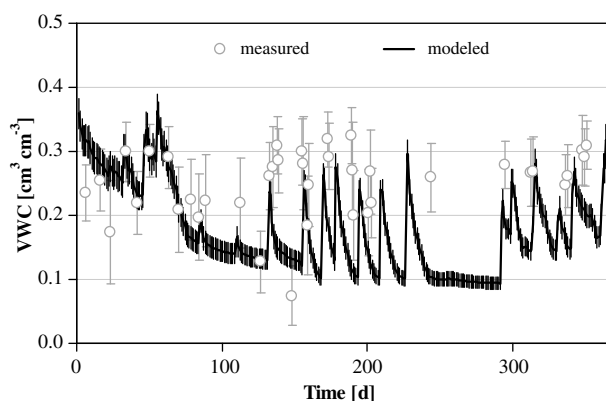


Figure 9 Volumetric water contents (VWC) ($\text{cm}^3 \text{ cm}^{-3}$) calculated using varied soil hydraulic properties (listed in Table 4). Error ranges (black shade) associated with simulated VWCs represent σ_{θ_w} .

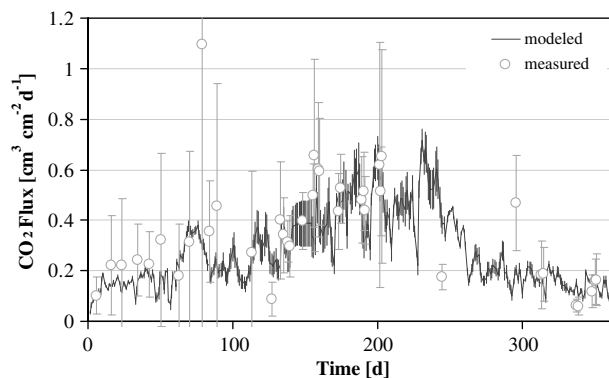


Figure 10 Simulated and measured CO₂ fluxes calculated using varied soil hydraulic properties (listed in Table 4). Error ranges (black shade) of simulated CO₂ fluxes represent σ_{q_c} .

altering the tortuosity factor and thus the effective gas diffusion coefficient. While soil temperatures affect significantly CO₂ production rates, different soil thermal parameters do not produce dramatically different soil temperatures at different depths. The effect of soil thermal parameters on CO₂ fluxes is thus smaller than the effect of soil hydraulic properties. Hence, uncertainties in the volumetric water content partly determine uncertainties in the CO₂ flux.

A moderate impact of soil hydraulic properties on CO₂ fluxes was found in the uncertainty analysis discussed above. This finding is consistent with the results presented in the previous section, where a dependency of model outputs on hydraulic properties and temperatures was observed. We found that error intervals associated with simulated and measured volumetric water contents (Fig. 9) are of the same order of magnitude. On the other hand, error intervals associated with simulated CO₂ fluxes are at least one order of magnitude smaller than error intervals of measured values. Hence, there are likely additional causes for the variability of CO₂ fluxes than those considered in our uncertainty analysis.

Summary and conclusions

The SOILCO₂ model was used in this study to evaluate soil CO₂ fluxes across multiple locations in an irrigated agricultural field in the Sacramento Valley, California. While soil hydraulic parameters were either estimated using neural network predictions from textural characteristics, or obtained as average values of a particular textural class, default values recommended by the HYDRUS-1D software were used for both heat and CO₂ transport and production parameters.

The results showed that the numerical model under predicted CO₂ fluxes between 16% and 32%. This seems to be acceptable since only limited soil information was used and the model was uncalibrated. A good level of correspondence between measured and simulated CO₂ fluxes with such limited information about model input parameters documents the applicability of the SOILCO₂ model to predict CO₂ fluxes from agricultural soils at the field scale.

A random value uncertainty analysis demonstrated that both simulated volumetric water contents and surface CO₂ fluxes show a relevant dependency on soil hydraulic properties. The variation of soil hydraulic properties led to uncertainty in volumetric water contents that was comparable to the uncertainty in measured CO₂ fluxes. The impact of heat transport parameters on surface CO₂ fluxes and volumetric water contents was noticeably smaller. We have observed an overall good performance of the SOILCO₂ model in predicting CO₂ fluxes from agricultural soils.

Acknowledgements

This research was partially supported by funding from the Kearney Foundation of Soil Science and the NSF biocomplexity program. We want to express our gratefulness to the reviewers and editors of *Journal of Hydrology*, who have made essential contributions by their outstanding reviews to develop this final version of the paper.

References

- Bauer, J., Herbst, M., Huisman, J.A., Weihermüller, L., Vereecken, H., 2008. Sensitivity of simulated soil heterotrophic respiration to choice of temperature and moisture reduction functions. *Geoderma* 145, 17–27.
- Buyanovski, G.A., Wagner, G.H., Gantzer, C.J., 1986. Soil respiration in a winter wheat ecosystem. *Soil Sci. Soc. Am. J.* 50, 338–344.
- Carsel, R.F., Parrish, R.S., 1988. Developing joint probability distributions of soil water retention characteristics. *Water Resour. Res.* 24, 755–769.
- Chung, S.-O., Horton, R., 1987. Soil heat and water flow with a partial surface mulch. *Water Resour. Res.* 23 (12), 2175–2186.
- Coleman, K., Jenkinson, D.S., 2005. RothC-26.3 A Model for Turnover of Carbon in Soil, Model Description and Windows Users Guide. IACR-Rothamsted, Harpenden, 45pp, <<http://www.rothamsted.bbsrc.ac.uk/aen/carbon/rothc.htm>>.
- Davidson, E.A., Janssens, I.A., 2006. Temperature sensitivity of soil carbon decomposition and feedbacks to climate change. *Nature* 440, 165–173.
- Dwyer, L.M., Ma, B.L., Stewart, D.W., Hayhoe, H.N., Balchin, D., Culley, J.L., McGovern, M., 1995. Root mass distribution under conventional and conservation tillage. *Can. J. Soil Sci.* 95 (01), 23–28.
- Fang, C., Moncrieff, J.B., 2001. The dependence of soil CO₂ efflux on temperature. *Soil Biol. Biochem.* 33, 155–165.
- Feddes, R.A., Kowalik, P.J., Zaradny, H., 1978. Simulation of Field Water Use and Crop Yield. Simulation Monographs. Pudoc, Wageningen.
- Franko, U., Crocker, G.J., Grace, P.R., Klir, J., Korschens, M., Poulton, P.R., Richter, D.D., 1997. Simulating trends in soil organic carbon in long-term experiments using the candy model. *Geoderma* 81, 109–120.
- Herbst, M., Hellebrand, H.J., Bauer, J., Huisman, J.A., Simunek, J., Weihermüller, L., Graf, A., Vanderborght, J., Vereecken, H., 2008. Multiyear heterotrophic soil respiration: evaluation of a coupled CO₂ transport and carbon turnover model. *Ecol. Model.* 214 (2), 271–283.
- Holt, J.A., Hodgen, M.J., Lamb, D., 1990. Soil respiration in the seasonally dry tropics near Townsville, North Queensland. *Aust. J. Soil Res.* 28, 737–745.
- Intergovernmental Panel on Climate Change, 2001. *Climate Change 2001: A Scientific Basis*. Cambridge University Press, Cambridge.
- Intergovernmental Panel on Climate Change, 2005. *Contribution of Working Group I to the Fourth Assessment Report of the Intergovernmental Panel on Climate Change, Summary for Policymakers*. Cambridge University Press, Cambridge.
- Lee, J., Six, J., King, A.P., van Kessel, C., Rolston, D.E., 2006. Tillage and field scale controls on greenhouse gas emissions. *J. Environ. Qual.* 35, 714–725.
- Lee, J., Rolston, D.E., Six, J., Hopmans, J., King, A., van Kessel, C., Paw, K.T., Plant, U.R., 2007. Predicting Changes in Landscape-Scale Soil Organic C Following the Implementation of Minimum Tillage. Research Report. Kearney Foundation of Soil Science, Davis, CA.
- Li, C., Frolking, S., Frolking, T.A., 1992. A model of nitrous oxide evolution from soil driven by rainfall events: 1. Model structure and sensitivity. *J. Geophys. Res.* 97 (D9), 9759–9776.
- Livingston, G.P., Hutchinson, G.L., Spartalian, K., 2005. Diffusion theory improves chamber-based measures of trace gas emissions. *Geophys. Res. Lett.* 32, L24817, doi:10.1029/2005GL024744.
- Livingston, G.P., Hutchinson, G.L., Spartalian, K., 2006. Trace gas emission in chambers: a non-steady-state diffusion model. *Soil Sci. Soc. Am. J.* 70, 1459–1469.
- Maas, E.V., 1990. *Crop Salt Tolerance in Agricultural Salinity Assessment and Management*. American Society of Civil Engineers, New York, NY.
- McConkey, B.G., Liang, B.C., Campbell, C.A., Curtin, D., Moulin, A., Brandt, S.A., Lafond, G.P., 2003. Crop rotation and tillage impact on carbon sequestration in Canadian prairie soils. *Soil Till. Res.* 74 (1), 81–90.
- Nielsen, D.R., Biggar, J.W., Erh, K.T., 1973. Spatial variability of field-measured soil-water properties. *Hilgardia* 42 (7), 215–259.
- Osher, L.J., Matson, P.A., Amundson, R., 2003. Effect of land use change on soil carbon in Hawaii. *Biogeochemistry* 65 (2), 213–232.
- Parkin, T.B., Kaspar, T.C., 2004. Temporal variability of soil carbon dioxide flux: effect of sampling frequency on cumulative carbon loss estimation. *Soil Sci. Soc. Am. J.* 68, 1234–1241.
- Parton, W.J., Schimel, D.S., Cole, C.V., Ojima, D.S., 1987. Analysis of factors controlling soil organic matter levels in the Great Plains grasslands. *Soil Sci. Soc. Am. J.* 51, 1173–1179.
- Parton, W.J., Stewart, J.W.B., Cole, C.V., 1988. Dynamics of C, N, P, and S in grassland soils: a model. *Biogeochemistry* 5, 109–131.
- Parton, W.J., Scurlock, J.M.O., Ojima, D.S., Gilmanov, T.G., Scholes, R.J., Schimel, D.S., Kirchner, T., Menaut, J.-C., Seastedt, T., Garcia-Moya, E., Apinan-Kamalrut, Kinyamario, J.I., 1993. Observations and modeling of biomass and soil organic matter dynamics for the grassland biome worldwide. *Global Biogeochem. Cy.* 7, 785–809.
- Patwardhan, A.S., Nieber, J.L., Moore, I.D., 1988. Oxygen, carbon dioxide, and water transfer in soils: mechanism and crop response. *Trans. ASEA* 31 (5), 1383–1395.
- Paustian, K., Six, J., Elliott, E.T., Hunt, H.W., 2000. Management options for reducing CO₂ emissions from agricultural soils. *Biogeochemistry* 48, 147–163.
- Poch, R.M., Hopmans, J.W., Six, J.W., Rolston, D.E., Mc Intyre, J.L., 2005. Considerations of a field-scale soil carbon budget for furrow irrigation. *Agric. Ecosyst. Environ.* 113 (1–4), 391–398.
- Post, W.M., Kwon, K.C., 2000. Soil carbon sequestration and land-use change: processes and potential. *Global Change Biol.* 6 (3), 317–327.
- Press, H.P., Teukolsky, S.A., Vetterling, W.T., Flannery, B.P., 1992. *Numerical Recipes in C*. Cambridge University Press, Cambridge, p. 289.

- Schaap, M.G., Leij, F.J., van Genuchten, M.Th., 2001. Rosetta: a computer program for estimating soil hydraulic parameters with hierarchical pedotransfer functions. *J. Hydrol.* 251, 163–176.
- Šimůnek, J., Suarez, D.L., 1993. Modeling of carbon dioxide transport and production in soil 1. Model development. *Water Resour. Res.* 29 (2), 499–513.
- Šimůnek, J., van Genuchten, M.Th., Šejna, M., 2005. The HYDRUS-1D Software Package for Simulating the One-Dimensional Movement of Water, Heat, and Multiple Solutes in Variably-Saturated Media. Version 3.0, HYDRUS Software Series 1. Department of Environmental Science, University of California Riverside, Riverside, California, p. 240.
- Smith, K.A., Ball, T., Conen, F., Dobbie, K.E., Massheder, J., Rey, A., 2003. Exchange of greenhouse gases between soil and atmosphere: interactions of soil physical factors and biological processes. *Eur. J. Soil Sci.* 54, 779–791.
- Soil Conservation Service, 1972. Soil Survey of Yolo County, California. Soil Conservation Service in Cooperation with University of California Agricultural Experiment Station. USDA, Washington, DC, pp. 93–96.
- Suarez, D.L., Šimůnek, J., 1993. Modeling of carbon dioxide transport and production in soil 2. Parameter selection, sensitivity analysis, and comparison of model predictions. *Water Resour. Res.* 29 (2), 499–513.
- Taylor, S.A., Ashcroft, G.M., 1972. *Physical Edaphology*. Freeman and Co., San Francisco, California.
- van Genuchten, M.Th., 1980. A closed-form equation for predicting the hydraulic conductivity of unsaturated soils. *Soil Sci. Soc. Am. J.* 44, 892–898.
- Williams, S.T., Shameemullah, M., Watson, E.T., Mayfield, C.I., 1972. Studies on the ecology of actinomycetes in soil, IV. The influence of moisture tension on growth and survival. *Soil Biol. Biochem.* 4, 215–225.
- Zak, D.R., Holmes, W.E., MacDonald, N.W., Pregitzer, K.S., 1999. Soil temperature, matric potential, and the kinetics of microbial respiration and nitrogen mineralization. *Soil Sci. Soc. Am. J.* 63, 575–584.
- Zhang, H., Pala, M., Oweis, T., Harris, H., 2000. Water use and water-use efficiency of chickpea and lentil in a Mediterranean environment. *Aust. J. Agric. Res.* 51, 295–304.